Bioorganic Chemistry 89 (2019) 103010

Contents lists available at ScienceDirect

Bioorganic Chemistry

journal homepage: www.elsevier.com/locate/bioorg

Molecular docking and experimental investigation of new indole derivative cyclooxygenase inhibitor to probe its binding mechanism with bovine serum albumin

Tanveer A. Wani[a,*], Ahmed H. Bakheit[a,b], Seema Zargar[c], Mashooq A. Bhat[a], Abdulrahman A. Al-Majed[a]

[a] Department of Pharmaceutical Chemistry, College of Pharmacy, King Saud University, P.O. Box 2457, Riyadh 11451, Saudi Arabia
[b] Department of Chemistry, Faculty of Science and Technology, Al-Neelain University, Khartoum, Sudan
[c] Department of Biochemistry, College of Science, King Saud University, PO Box 22452, Riyadh 11451, Saudi Arabia

ABSTRACT

The indole derivative 2-(5-methoxy-2-methyl-1H-indol-3-yl)-N'-[(E)-(3-nitrophenyl) methylidene]acetohydrazide (IND) was synthesized for its therapeutic potential to inhibit cyclooxygenase (COX)-II. Binding if IND to bovine serum albumin (BSA) was investigated was because most drugs bind to serum albumin *in*-vivo. Fluorescence, UV–vis spectrophotometry and molecular modeling methodologies were employed for studying the interaction mechanism. The intrinsic fluorescence of BSA was quenched by BSA and the quenching mechanism involved was static quenching. The binding constants between IND and BSA at the three studied temperatures (298, 301 and 306 K) were 1.09×10^5, 4.36×10^4 and 1.23×10^4 L mol^{-1} respectively. The most likely site for binding IND to BSA was Site I (subdomain IIA). The analysis of thermodynamic parameter revealed the involvement of hydrogen bonding and van der Waals forces in the IND-BSA interaction. Synchronous fluorescence spectroscopic (SFS) and UV–vis spectrophotometric studies suggested conformational change in BSA molecule post interaction to IND. Molecular docking and the experimental results corroborated one another. The study can prove as an insight for future IND drug development.

1. Introduction

During the palliative care the patients are provided with analgesics which consist of non-steroidal anti-inflammatory drugs (NSAIDs). The use of NSAIDs leads to several adverse events and the most common among them is gastrointestinal (GI) morbidity that include both upper and lower GI complications [1,2]. The pharmacological activity of NSAIDs depends on its capability to inhibit the COX enzymes that exist as isoform COX-I and COX-II [3]. Most tissues express COX-I isoform, which play a protective role by producing prostaglandins. The prostaglandins stimulate the synthesis and secretion of mucus and bicarbonate, surge mucosal blood flow and promote epithelial proliferation. The inflammatory stimuli cause induction of COX-II in the inflammatory cells and help in prostaglandin biosynthesis. The inhibition of COX-I in particular is responsible for the gastric ulcer formation than COX-II [3,4]. The limitation to the long term use of these selective COX-II inhibitors being ulcer exacerbations and other systemic side effects. These side effects have led to withdrawal of certain COX-II inhibitors and have also necessitated the need for synthesis of new and safer NSAIDs.

Chemical alteration of indomethacin improves its safety profile and increases its anti-inflammatory activity with a decrease in ulcerogenicity. The chemical modification of indomethacin provided an indole derivative having COX-2 inhibitor activity with anti-inflammatory and analgesic properties. The synthesized indole derivative 2-(5-methoxy-2-methyl-1H-indol-3-yl)-N'-[(E)-(3-nitrophenyl) methylidene] acetohydrazide (IND) has COX-II inhibiting properties (Fig. 1), [M.p.: 200–202 °C; IR (KBr) cm^{-1}: 3412 (NH), 3237 (C–H), 1654 (C=O), 1640 (C=O), 1617 (C=n); 1H NMR (500 MHz, DMSO-d_6) δ ppm: 1.3 (3H, s, $-CH_3$), 3.58 (2H, s, CH_2), 3.74 (3H, s, $-OCH_3$), 6.99–8.57 (7H, m, Ar–H), 10.63 (1H, s, =CH), 11.5 (1H, s, NH, D_2O exchg.), 12.18 (1H, s, $-CONH$, D_2O exchg.); ^{13}C NMR (125 MHz DMSO-d_6) δ = 11.59, 27.92, 55.02, 55.34, 100.27, 103.95, 109.49, 120.72, 123.81, 124.24, 128.57, 129.61, 130.0, 131.73, 132.78, 133.09, 136.05, 140.33,145.57, 148.14, 152.87, 153.01, 162.27, 167.69; MS: m/z = 366.37 [M] +; Analysis: for $C_{19}H_{18}N_4O_4$, calcd. C, 62.29; H, 4.93; N, 15.24%. Anti-inflammatory, analgesic and ulcerogenic potential of IND has been studied and has been reported to have reduced ulcer index [5,6].

Protein binding studies have been used to investigate the mechanism of binding interactions, changes in structural conformations and stability of proteins upon interactions with ligands. [7,8]. Various proteins have been studied using spectroscopic approaches for their interaction with ligands [7–10]. Serum albumin acts as a carrier protein

* Corresponding author.
E-mail address: twani@ksu.edu.sa (T.A. Wani).

https://doi.org/10.1016/j.bioorg.2019.103010
Received 27 November 2018; Received in revised form 21 March 2019; Accepted 21 May 2019
Available online 22 May 2019
0045-2068/

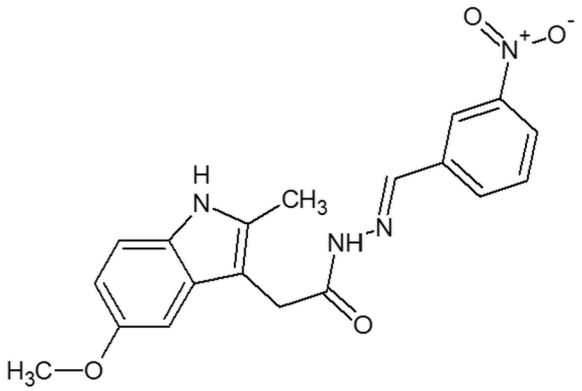

Fig. 1. Chemical structure of indole derivative 2-(5-methoxy-2-methyl-1H-indol-3-yl)-N'-[(E)-(3-nitrophenyl) methylidene] acetohydrazide (IND).

for transportation of various endogenous and exogenous molecules including drug ligands [10–13]. Bovine serum albumin was selected as interaction protein due to its structural analogy to human serum albumin. BSA has been widely studied for its binding interaction with drug moieties [14]. The drug ligands usually are small organic molecules and these interact with the basic amino acid residues of proteins. The interaction studies give an insight regarding the *in-vivo* drug pharmacological properties. [13,15,16]. Therefore, the investigation of the coupling between BSA and drug ligands are extensively studied by scientists [15–20]. *In vivo* binding interactions are difficult and the fluorescence spectroscopy has considerably helped in exploring these binding interactions *in vitro*.

The aim of this binding interaction study between IND and BSA was to understand the mechanism involved and provide an insight for pharmacological development of IND. To attain the purpose several experimental studies that included fluorescence, UV absorbance, site marker completion and molecular docking were employed.

2. Experimental

2.1. Reagents

The chemicals were procured from the following sources: BSA (Sigma Aldrich; USA). IND was synthesized in-house in the medicinal chemistry laboratory of the pharmaceutical chemistry department [5]. Phenylbutazone and Ibuprofen were procured through National Scientific Company; Saudi Arabia.

2.2. Absorbance measurements

The absorbance spectra were recorded with UV spectrophotometer (UV-1800 from Shimadzu Japan). The spectra were recorded at room temperature and in the range of 200–400 nm for BSA and BSA-IND complexes.

2.3. Inner filter effect correction

The inner filter effect that could be encountered during the IND and BSA fluorescence spectral measurements were corrected with:

$$Fcor = Fobs \times e^{(Aex+Aem)/2}$$

where F_{cor} and F_{obs} are the fluorescence intensity (FI) after and before the correction. A_{ex} and A_{em} are the absorbances at the excitation and emission, respectively.

2.4. Fluorescence measurements

Fluorescence spectra were acquired with Jasco spectrofluorometric (JASCO FP-8200; Easton, USA). The fluorescence spectra were acquired at λ_{ex} 280 nm and λ_{em} 300–500 nm. The BSA concentration was constant throughout the experiment at 1.5 μM. An equal volume of IND with concentrations ranging from (1.53×10^{-6} M − 2.45×10^{-5} M) were added to the BSA solution [17,18]. The actual analyzed sample concentrations were 0.75×10^{-6} M for BSA solution and (7.64×10^{-7}, 1.53×10^{-6}, 3.06×10^{-6}, 6.11×10^{-6}, 9.17×10^{-6} and 1.22×10^{-5} M) for IND. The sample mixtures were prepared in phosphate buffer saline (PBS) pH 7.40. The synchronous fluorescence spectra (SFS) at intervals $\Delta\lambda = 15$ and 60 nm ($\Delta\lambda = \lambda em - \lambda ex$) were acquired for BSA and BSA-IND complexes at room temperature. The acquired spectra at $\Delta\lambda = 15$ and $\Delta\lambda = 60$ nm provided characteristics of tyrosine (Tyr) that of tryptophan (Trp) residues, respectively. Three dimensional (3D) fluorescence spectroscopy is believed to be more specific methodology in understanding the fluorescence chromophore behavior. It also helps to establish any conformational changes in the protein due to protein –ligand interaction.

2.5. Site marker competitive fluorescence experiments

The binding site identification studies for BSA-IND were performed with phenylbutazone (site I) and ibuprofen (site II). Equal volumes of BSA (1.5 μM) and phenylbutazone (1.6×10^{-6} M) or ibuprofen (4.3×10^{-6} M) in PBS pH 7.4 were mixed and incubated together. Different IND concentrations were added to these incubated samples and the fluorescence spectra recorded.

2.6. Fluorescence resonance energy transfer (FRET)

The FRET is used in determination of any energy transfer that might have occurred. In this interaction BSA acts as donor and IND as acceptor. FRET occurs due to an overlap in the donor emission spectrum and acceptor absorption spectrum. The FRET is calculated by Forster theory [12].

2.7. Molecular docking

The mode of binding between IND and BSA was investigated by molecular docking (Molecular Operating Environment; MOE). The three dimensional BSA crystal structure, Code No. of 4OR0; was attained from Protein Data Bank (http://www.rcsb.org/pdb). The IND structure was drawn with MOE software. The energy was optimized by default force field MMFF94X method while the RMS gradient was kept at 0.05 kcal mol^{-1}. The rescoring function 1 and 2 were London dG and GBVI/WSA dG, respectively. The selection for binding site on BSA was performed as per the results from the site probe experiments.

3. Results and discussion

3.1. Fluorescence quenching analysis

The study of binding interaction of drugs to proteins with fluorescence spectroscopy has emerged as a powerful tool owing to its sensitivity, accuracy and ease of use [21–23]. Endogenous fluorophore residues Trp and Tyr in BSA are responsible for its fluorescent nature. The fluorescence spectra were measured at three different temperatures of 298, 301 and 306 K and FI at 298 K was the highest. As the concentration of IND was increased in the BSA-IND complex as decrease in the FI of BSA was observed. The basic peak shape didn't alter, however, a red shift was observed at λ_{em}, suggesting BSA-IND of a complex formation (Fig. 2). Further, occurrence of a shift in the λ_{em}, indicates the existence of hydrophobic amino acids or polar groups within the fluorophore microenvironment [24,25]. The two different types of quenching mechanisms involved in the fluorescence quenching process are static and dynamic quenching. Dynamic quenching is exhibited when the intermolecular collision amongst the quencher and the

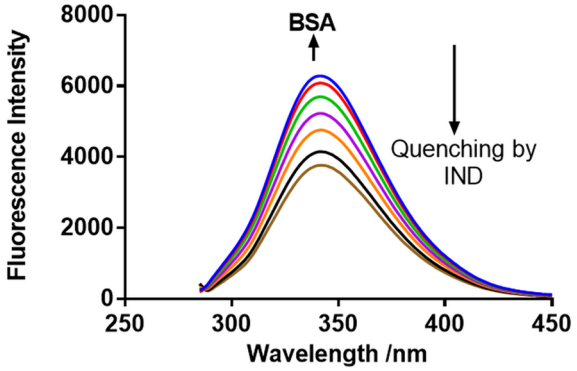

Fig. 2. Fluorescence of spectra BSA in absence and presence of different concentrations of IND at 298 K.

fluorescent molecule occur at an excited state. The structure or activity of a protein are independent of the dynamic quenching. The intramolecular interaction at ground state amongst the fluorescent molecule and quencher leads to static quenching. In static quenching process, creation of a new composite occurs and the newly formed composite is unstable at high temperatures. The reason behind the decreased steadiness is attributed to the high molecular diffusion, since, the weakly bound composites can get dissociated at high temperatures. Thus, the responses of the processes with temperature help in establishing the quenching mechanism involved. Stern-Volmer equation was employed to identify the type of quenching mechanism in the interaction of BSA-IND [25,26]:

$$\frac{F_0}{F} = 1 + K_{sv}[Q] = 1 + K_q \tau_0 [Q]$$

The FI in absence and in presence of quencher are designated by F_0 and F, respectively. τ_0 is the lifetime of fluorescent molecule without of quencher and is valued 10^{-8} s [27]. K_{sv} is the Stern-Volmer quenching rate constant ($K_{sv} = K_q\ \tau_0$) whereas, K_q and [Q] represents the quenching rate constant and quencher concentration, respectively. A maximum value of $2 \times 10^{10}\,M^{-1}\,S^{-1}$ can be achieved for quenching constant in case of biopolymers [26]. However, the K_{sv} values obtained during this study at the studied temperatures were greater than the maximum value specifying contribution of static quenching in IND- BSA interaction (Table 1). Further, a decrease in the K_{sv} values with increase in temperature also indicates static quenching mechanism. The K_{sv} is determined from the slope of linear regression plot of F_0/F and [Q] (Fig. 3A) and supports the theory that static quenching is involved in the interaction.

3.2. Binding constants, sites and forces between IND and BSA

A higher binding constant ($> 10^4\,L\,mol^{-1}$) is observed in cases of high binding affinity, whereas, binding constant ($< 10^3\,L\,mol^{-1}$) indicate low affinity [28]. The binding constant (K_b) was from determined as:

$$\log\frac{(F_0 - F)}{F} = \log K_b + n\log[Q]$$

The binding constant "K_b" and binding site number "n" are determined respectively, from the intercept and slope of double logarithm regression plot between log [(F_0-F))/F] and log [Q]. The binding constants (K_b) attained at the three studied temperatures (298, 301 and 306 K) were between 1.09×10^5–$1.23 \times 10^4\,L\,mol^{-1}$ with binding site number equivalent to 1 (Table 2) (Fig. 3B). The high binding constant values obtained with BSA and IND interaction indicate a very strong binding interaction between them. Therefore, it is expected that IND will strongly bind to plasma proteins *in*-vivo. Also it was observed that at higher temperatures the binding constants decreased suggesting instability of the complex at high temperature [29].

Table 1
BSA Stern–Volmer quenching constants (K_{SV}) and quenching rate constant (Kq) in presence of IND at different temperatures.

T (K)	R	$K_{sv} \pm SD \times 10^4$ ($L\,mol^{-1}$)	$K_q \times 10^{12}$ ($L\,mol^{-1}\,s^{-1}$)
298	0.9982	5.51 ± 0.32	5.51×10^{12}
301	0.9940	5.32 ± 0.19	5.32×10^{12}
306	0.9774	4.59 ± 0.23	4.59×10^{12}

3.3. Identification binding sites for IND

Site competition experiments were done to recognize the sites of BSA that bind IND. To accomplish these experiments, site markers phenylbutazone (PBT) site I and ibuprofen (IBF) site II were used (Fig. 3C). The FI of BSA decreased after addition of IND to the mixture of BSA–PBT or BSA–IBF. The binding constants were calculated for both BSA– PBT or BSA– IBF with IND and compared to that attained in absence of the site markers. For the PBT and IBF mixtures the binding constants were found to be 0.99×10^2 and 2.89×10^3, respectively, and suggests a competition interaction amongst IND and PBT with BSA. The binding constant of BSA in presence of PBT and IBF decreased from binding constant 1.09×10^5 found for BSA-IND complex. However, the decrease in the PBT complex was far greater than IBF suggesting binding of IND binds mainly to site I but involvement of site II in binding IND cannot be ruled out.

3.4. Binding forces involved IND and BSA interaction

The proteins and ligands binding interaction might involve different types molecular forces. These binding forces may include the hydrogen bonds, van der Waals forces, electrostatic forces and hydrophobic interactions [30,31]. The binding modes are confirmed enthalpy ΔH° and entropy ΔS° change which act as indicators for forces responsible for the interaction. The negative values of ΔH° and ΔS° both, indicates hydrogen bonds and/or van der Waals forces. The electrostatic forces are inferred in case the ΔH° takes a negative value and ΔS° a positive value. The hydrophobic interaction is suggested in case both ΔH° and ΔS° take a positive value [31,32]. The following equation was used for the thermodynamic parameter calculation:

$$\ln Kb = -\frac{\Delta H^\circ}{RT} + \frac{\Delta S^\circ}{R}$$

$$\Delta G^\circ = \Delta H^\circ - T\Delta S^\circ = -RT\ln Kb$$

where K_b is binding constant; R universal gas constant. van't Hoff plot for the BSA and IND interaction is given in Fig. 3D. The free energy change (ΔG°) attained negative values (Table 2) representing a spontaneous binding between BSA and IND. Further, both the ΔH° and ΔS° attained negative values indicating that hydrogen bonding and van der Waals forces to be the main forces involved in the BSA-IND interaction. From the thermodynamic results it is suggested that BSA and IND interaction is enthalpy driven as the entropy attained negative value in this interaction.

3.5. Energy transfer from BSA to IND

UV-absorption spectroscopy of IND showed a weak absorption in the fluorescence emission spectral range (300–500 nm) of BSA. A spectral overlap in the BSA emission spectrum and IND absorption spectrum was are presented in Fig. 4. An overlap in the fluorescence emission spectrum of BSA and the absorption spectrum of spectrum of IND suggests a possibility for FRET.

The critical energy transfers distance (R_0) and the efficiency (E) of energy transfer are attained from the integral overlap region of donor

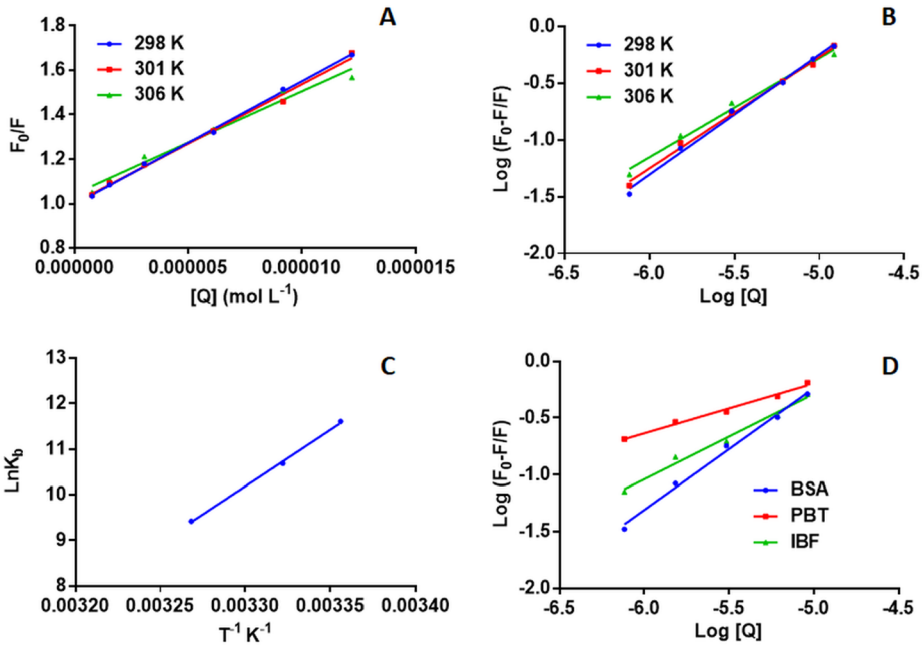

Fig. 3. [A]: The stern–Volmer curves for the quenching of BSA by IND at 298/301/306 K; [B]: The plot of log $[(F_0 - F)/F]$ versus log[Q] for quenching process of IND with BSA at 298/301/306 K; [C]: Van't Hoff plots for the binding interaction of IND with BSA; [D]: The plot of log $[(F_0 - F)/F]$ versus log[Q] for quenching process of IND with BSA in presence of site markers phenylbutazone and ibuprofen at 298 K.

Table 2
Calculated binding constant values and thermodynamic parameters of binding between IND and BSA.

T (K)	R	$K_b \pm SD \times 10^5$ (L mol^{-1})	n	ΔG° (kJ mol^{-1})	ΔH° (kJ mol^{-1})	ΔS° (J mol^{-1} K^{-1}
298	0.9946	10.9 ± 0.37	1.06	−27.93	−172	−485
301	0.9956	4.36 ± 0.19	0.9826	−26.48		
306	0.9901	1.23 ± 0.07	0.8742	−24.05		

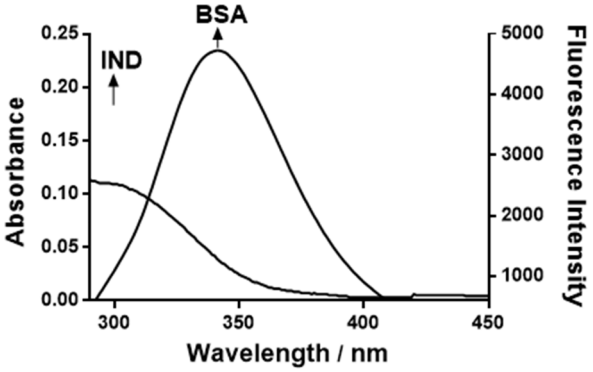

Fig. 4. Spectral overlap of donor BSA (fluorescence spectrum) with acceptor **IND** (absorption spectrum).

(BSA) and acceptor (IND) using Forster equation [26].

$$E = 1 - \frac{F_0}{F} = \frac{R_0^6}{R_0^6 + r^6}$$

where F_0 and F are the FI of BSA in absence and presence of IND. 'r' is the donor/acceptor binding distance. The critical binding distance is obtained from:

$$R_0^6 = 8.79 \times 10^{-25}\ K^2 \phi_D n^{-4} J$$

where spatial orientation factor of the dipole is specified as K^2; n is refractive index of medium; Φ_D quantum yield of the donor in acceptors absence; and J represents integral overlap between emission and absorption spectrum and is given as:

$$J(\lambda) = \frac{\sum F(\lambda) \in (\lambda)\lambda^4 \Delta\lambda}{\sum (\lambda)\Delta\lambda}$$

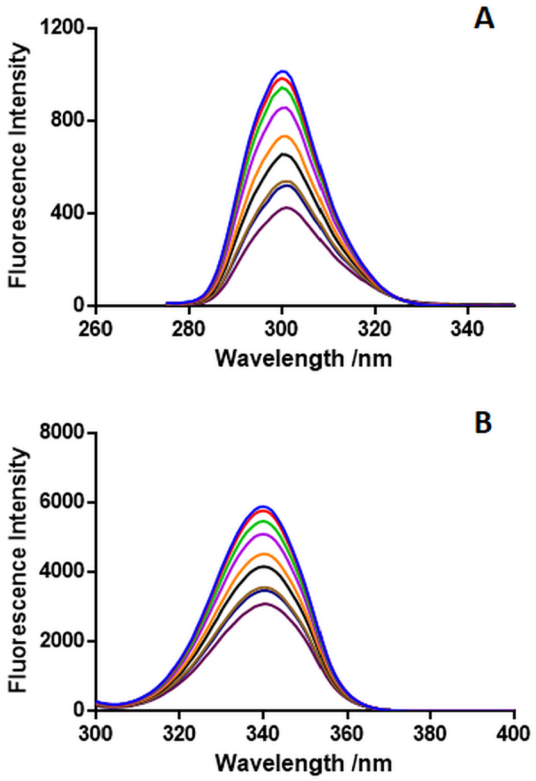

Fig. 5. Synchronous fluorescence spectroscopic data of BSA in presence of IND at 298 K [A] $\Delta\lambda$ = 15 nm and [B] $\Delta\lambda$ = 60 nm.

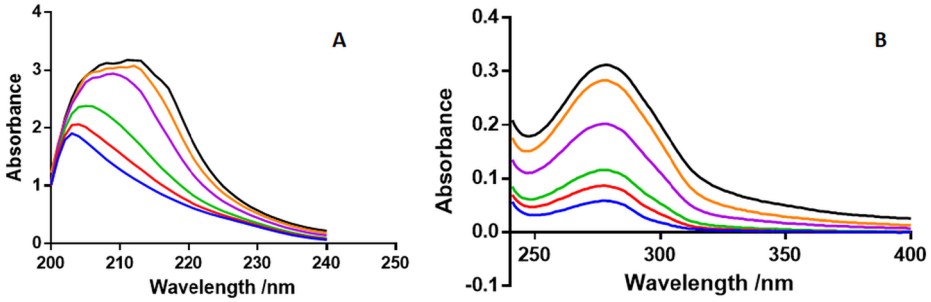

Fig. 6. UV-Absorption spectra of BSA in presence and absence of IND.

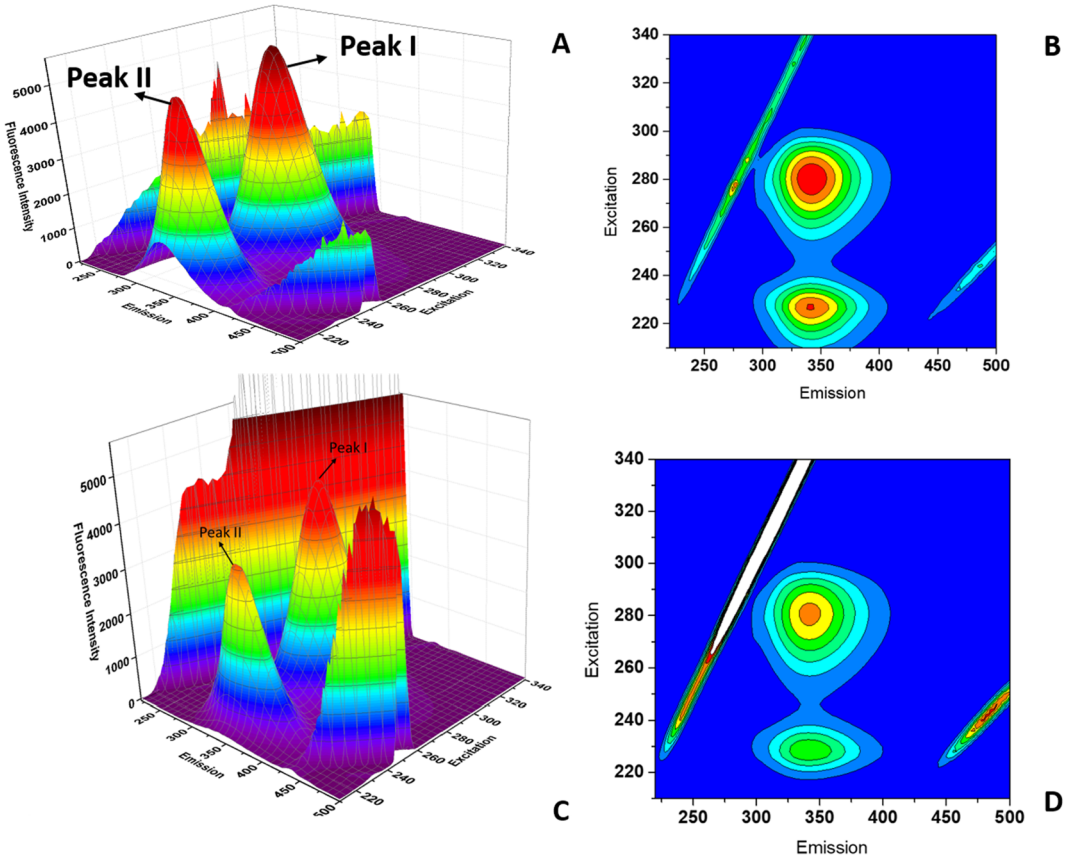

Fig. 7. Three dimensional fluorescence analysis and contour plot for BSA [A and B]: BSA and BSA-IND complex [C and D].

where F(λ) is FI of donor, ε(λ) is the molar absorptivity of acceptor.

The K^2, n and Φ_D were 2/3, 1.336 and 0.118, respectively for this study and the calculated values for E, R_0 and J(λ) were found to be 0.0381, 1.90 and 2.13 × 10^{-15}. Thus, the calculated binding distance 'r' between BSA and IND was 3.08 nm. The obtained binding distance was within the limit of up to 2–8 nm for effective non-radiative energy transfer between BSA and IND. Thus, it was inferred that energy transfer ensued amongst BSA and IND and the fluorescence quenching mechanism for BSA-IND interaction was static in nature.

3.6. Synchronous fluorescence spectroscopy

The micro-environmental changes around the amino acid residues are detected by SFS. Shift the maximum λ_{em} indicates changes the micro-environment of amino acids and the polarity of chromosphere molecules. Tyrosine and tryptophan are primarily responsible for the BSA fluorescence. The characteristic information of tyrosine and tryptophan residues is provided at Δλ = 15 nm and Δλ = 60 nm respectively [33–35]. A reduction in FI occurred at Δλ = 15 nm which was further reduced as the IND concentration increased with a shift of 1 nm (redshift) in λ_{em} (Fig. 5) indicating decreased hydrophobicity and increased stretching capacity of the peptide chain. The reduction in FI at Δλ = 60 nm was greater than that was detected at Δλ = 15 nm without any shift in λ_{em} [34,35].

3.7. UV–vis absorption studies

These studies provide facts for any structural changes and complex formation occurring in the ligand and protein interaction. As is evident from Fig. 6, the absorption of samples increased as the concentrations of IND increased (BSA fixed concentration). Based on these observations it is suggested that a complex formation between BSA and IND led to increase in the absorption of BSA [36–37].

3.8. Three dimensional fluorescence spectroscopy

The conformational changes in the proteins can be detected by three dimensional fluorescence spectroscopy [36]. The three dimensional

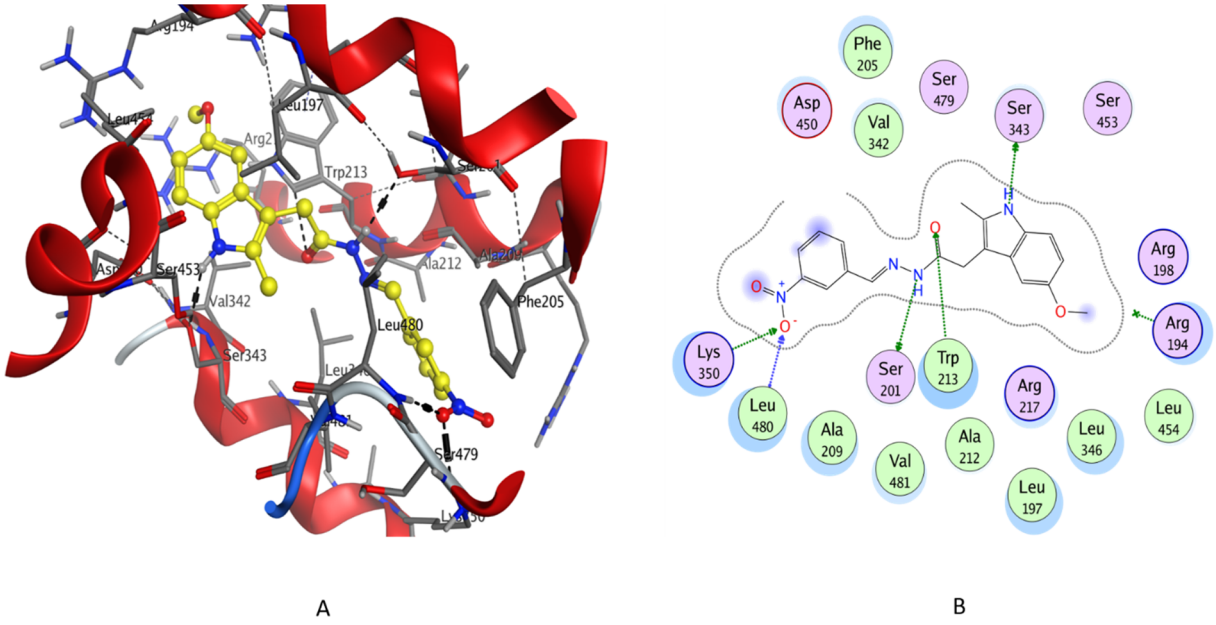

Fig. 8. [A] The docking conformation of IND-BSA complex with lowest energy. [B] The amino acid residues surrounding IND.

spectra and contour plots are presented in Fig. 7. Peak I which is the strongest peak at λ_{ex} = 280 nm, λ_{em} = 340 nm primarily divulges the amino acid residue Trp behavior. In addition to peak I another strong peak (peak II) occurs at λ_{ex} = 230 nm, λ_{em} = 340 nm and provides information about the polypeptide backbone structure events. The intensity of fluorescence reduced upon addition of IND also peak I part of contour spectra transformed to be sparse. This reduction on the FI clearly indicates conformational and micro-environmental changes in BSA upon addition of IND due to complex formation between BSA and IND.

3.9. Molecular docking

Molecular docking along with experimental results help in understanding the IND and BSA interaction (Fig. 8A) [22]. The molecular docking confirmed the experimental findings of the binding site for IND being at site I of BSA. The theoretical free binding energy of the BSA with IND from the molecular docking analysis was found to be $-28.28\ kj\ mol^{-1}$ and is closer the binding energy of $-27.93\ kj\ mol^{-1}$ obtained experimentally.

Fig. 8B also indicates that the IND molecule is embedded in the hydrophobic region of subdomain IIA of BSA. IND is encircled by the hydrophobic amino acid residues of Ala-212, Ala-209, Leu-454, Leu-346, Leu-480, Leu-197, Val-342, Val-481, Phe-205 polar residues like Trp-213, Ser-453, Ser-343, Ser-201, Ser-479 and charge residues such as Arg-217, Arg-198, Arg-194, Asp-450, Lys-450. Hydrogen bonding interactions are amongst IND and BSA were observed at Trp-453, Ser-201, Lys-350, Arg-194 and Ser-343. The thermodynamic studies also indicated that hydrogen bonding and van der Waals forces contributed to the BSA-IND interaction.

4. Conclusion

IND has been patented with the USPTO as COX-II inhibitor and its in-vitro protein (BSA) interaction was comprehended in this study. The binding site and docking studies revealed site I (subdomain IIA) was predominantly involved in binding IND to BSA molecule. The static quenching in BSA-IND interaction indicated a new composite formation among them. Further, a conformational change in BSA was proposed on the basis of SFS and UV spectroscopic analysis. Hydrogen bonds and van der Waals forces were suggested in the interaction and was enthalpy driven. The study will be helpful in preclinical drug developmental studies of IND.

Acknowledgments

The authors would like to extend their sincere appreciation to the Deanship of Scientific Research, King Saud University, for funding the research group No. RG-1435-073.

Declaration of Competing Interest

The authors declare that they have no competing interests.

Appendix A. Supplementary material

Supplementary data to this article can be found online at https://doi.org/10.1016/j.bioorg.2019.103010.

References

[1] P. Sharma, N. Rane, V. Gurram, Synthesis and QSAR studies of pyrimido [4, 5-d] pyrimidine-2, 5-dione derivatives as potential antimicrobial agents, Bioorg. Med. Chem. Lett. 14 (16) (2004) 4185–4190.
[2] N. Agarwal, S.K. Raghuwanshi, D. Upadhyay, P. Shukla, V.J. Ram, Suitably functionalised pyrimidines as potential antimycotic agents, Bioorg. Med. Chem. Lett. 10 (8) (2000) 703–706.
[3] V. Ram, N. Haque, P. Guru, Chemotherapeutic agents XXV: synthesis and leishmanicidal activity of carbazolylpyrimidines, Eur. J. Med. Chem. 27 (1992) 851–855.
[4] S. Vega, J. Alonso, J.A. Diaz, F. Junquera, Synthesis of 3-substituted-4-phenyl-2-thioxo-1, 2, 3, 4, 5, 6, 7, 8-octahydrobenzo [4, 5] thieno [2, 3-á] pyrimidines, J. Heterocycl. Chem. 27 (2) (1990) 269–273.
[5] A. Al-Dhfyan, M.A. Bhat, US Patent 9 (2015) 119–856.
[6] F. Shakeel, M.A. Bhat, N. Haq, Solubility and thermodynamics of 4-(4-ethoxyphenyl)-5-(3, 4, 5-trimethoxybenzoyl)-3, 4-dihydropyrimidin-2 (1H)-one in various pure solvents at different temperatures, J. Mol. Liq. 224 (2016) 624–628.
[7] J. Chamani, Comparison of the conformational stability of the non-native α-helical intermediate of thiol-modified β-lactoglobulin upon interaction with sodium n-alkyl sulfates at two different pH, J. Colloid. Interface Sci. 299 (2) (2006) 636–646.
[8] M. Ghaderabad, M. Mansouri, S. Beigoli, A.S. Rad, J. Mehrzad, M.R. Saberi, J. Chamani, A comparison of the inclusion behavior of human serum albumin and holo transferrin with fluoxymesterone in the presence of three different cyclodextrins, J. Iran. Chem. Soc. 14 (7) (2017) 1347–1364.
[9] S. Sharif-Barfeh, S. Beigoli, A.S. Marouzi, A. Rad, J. Asoodeh, Chamani, Multispectroscopic and HPLC studies of the interaction between estradiol and cyclophosphamide with human serum albumin: binary and ternary systems, J. Solu. Chem. 46 (2) (2017) 488–504.

[10] B. Bakaeean, M. Kabiri, H. Iranfar, M.R. Saberi, J. Chamani, Binding effect of common ions to human serum albumin in the presence of norfloxacin: investigation with spectroscopic and zeta potential approaches, J. Solu. Chem. 41 (10) (2012) 1777–1801.
[11] S. Curry, H. Mandelkow, P. Brick, N. Franks, Crystal structure of human serum albumin complexed with fatty acid reveals an asymmetric distribution of binding sites, Nat. Struct. Biol 5 (9) (1998) 827.
[12] S. Ranjbar, Y. Shokoohinia, S. Ghobadi, N. Bijari, S. Gholamzadeh, N. Moradi, M.R. Ashrafi-Kooshk, A. Aghaei, R. Khodarahmi, Studies of the interaction between isoimperatorin and human serum albumin by multispectroscopic method: identification of possible binding site of the compound using esterase activity of the protein, Sci. World. J. 2013 (2013), https://doi.org/10.1155/2013/305081.
[13] J. Simard, P. Zunszain, C.E. Ha, J. Yang, N. Bhagavan, I. Petitpas, S. Curry, J. Hamilton, Locating high-affinity fatty acid-binding sites on albumin by x-ray crystallography and NMR spectroscopy, Proc. Natl. Acad. Sci. USA 102 (50) (2005) 17958–17963.
[14] X.M. He, D.C. Carter, Atomic structure and chemistry of human serum albumin, Nature 358 (6383) (1992) 209.
[15] T.A. Wani, A.H. Bakheit, A.-R.A. Al-Majed, M.A. Bhat, S. Zargar, Study of the interactions of bovine serum albumin with the new anti-inflammatory agent 4-(1, 3-Dioxo-1, 3-dihydro-2H-isoindol-2-yl)-N′-[(4-ethoxy-phenyl) methylidene] benzohydrazide using a multi-spectroscopic approach and molecular docking, Molecules 22 (8) (2017) 1258.
[16] T.A. Wani, A.H. Bakheit, S. Zargar, M.A. Hamidaddin, I.A. Darwish, Spectrophotometric and molecular modelling studies on in vitro interaction of tyrosine kinase inhibitor linifanib with bovine serum albumin, PloS one 12 (4) (2017) e0176015.
[17] A. Jahanban-Esfahlan, V. Panahi-Azar, S. Sajedi, Spectroscopic and molecular docking studies on the interaction between N-acetyl cysteine and bovine serum albumin, Biopolymers 103 (11) (2015) 638–645.
[18] S. Khorsand Ahmadi, M. Mahmoodian Moghadam, P. Mokaberi, M. Reza Saberi, J. Chamani, A comparison study of the interaction between β-lactoglobulin and retinol at two different conditions: spectroscopic and molecular modeling approaches, J. Biomol. Struct. Dyn. 33 (9) (2015) 1880–1898.
[19] S. Marouzi, A.S. Rad, S. Beigoli, P.T. Baghaee, R.A. Darban, J. Chamani, Study on effect of lomefloxacin on human holo-transferrin in the presence of essential and nonessential amino acids: Spectroscopic and molecular modeling approaches, Int. J. Biol. Macromol. 97 (2017) 688–699.
[20] J. Chamani, M. Heshmati, Mechanism for stabilization of the molten globule state of papain by sodium n-alkyl sulfates: spectroscopic and calorimetric approaches, J. Colloid. Interface. Sci. 322 (1) (2008) 119–127.
[21] T.A. Wani, A.H. Bakheit, M.N. Ansari, A.-R.A. Al-Majed, B.M. Qahtani, S. Zargar, Spectroscopic and molecular modeling studies of binding interaction between bovine serum albumin and roflumilast, Drug Des. Develop. Ther. 12 (2018) 2627–2634.
[22] Y.-C. Chen, H.-M. Wang, Q.-X. Niu, D.-Y. Ye, G.-W. Liang, Binding between saikosaponin C and human serum albumin by fluorescence spectroscopy and molecular docking, Molecules 21 (2) (2016) 153.
[23] M. Möller, A. Denicola, Protein tryptophan accessibility studied by fluorescence quenching, Biochem. Mol. Biol. Educ. 30 (3) (2002) 175–178.
[24] B.E. Cohen, A. Pralle, X. Yao, G. Swaminath, C.S. Gandhi, Y.N. Jan, B.K. Kobilka, E.Y. Isacoff, L.Y. Jan, A fluorescent probe designed for studying protein conformational change, Proc. Natl. Acad. Sci. USA 102 (4) (2005) 965–970.
[25] A. Moosavi-Movahedi, M. Gharanfoli, K. Nazari, M. Shamsipur, J. Chamani, B. Hemmateenejad, M. Alavi, A. Shokrollahi, M. Habibi-Rezaei, C. Sorenson, A distinct intermediate of RNase A is induced by sodium dodecyl sulfate at its pK a, Colloids Surf. B. Biointerf. 43 (3) (2005) 150–157.
[26] J. Kang, Y. Liu, M.-X. Xie, S. Li, M. Jiang, Y.-D. Wang, Interactions of human serum albumin with chlorogenic acid and ferulic acid, Biochim. Biophys. Acta 1674 (2) (2004) 205–214.
[27] J. Chamani, H. Vahedian-Movahed, M.R. Saberi, Lomefloxacin promotes the interaction between human serum albumin and transferrin: a mechanistic insight into the emergence of antibiotic's side effects, J. Pharm. Biomed. Anal. 55 (1) (2011) 114–124.
[28] M.M. Moghaddam, M. Pirouzi, M.R. Saberi, J. Chamani, Comparison of the binding behavior of FCCP with HSA and HTF as determined by spectroscopic and molecular modeling techniques, Luminescence 29 (4) (2014) 314–331.
[29] M.R. Housaindokht, J. Chamani, A.A. Saboury, A.A. Moosavi-Movahedi, M. Bahrololoom, Three binding sets analysis of alpha-Lactalbumin by interaction of tetradecyl trimethyl ammonium bromide, Bull. Korean Chem. Soc. 22 (2) (2001) 145–148.
[30] J. Tian, J. Liu, W. He, Z. Hu, X. Yao, X. Chen, Probing the binding of scutellarin to human serum albumin by circular dichroism, fluorescence spectroscopy, FTIR, and molecular modeling method, Biomacromolecules 5 (5) (2004) 1956–1961.
[31] I.M. Klotz, J.M. Urquhart, The binding of organic ions by proteins. Effect of temperature, J. Am. Chem. Soc. 71 (3) (1949) 847–851.
[32] P.D. Ross, S. Subramanian, Thermodynamics of protein association reactions: forces contributing to stability, Biochemistry 20 (11) (1981) 3096–3102.
[33] J. Benesch, G. Hungerford, K. Suhling, C. Tregidgo, J.F. Mano, R.L. Reis, Fluorescence probe techniques to monitor protein adsorption-induced conformation changes on biodegradable polymers, J. Colloid. Interface Sci. 312 (2) (2007) 193–200.
[34] M. Zolfagharzadeh, M. Pirouzi, A. Asoodeh, M.R. Saberi, J. Chamani, A comparison investigation of DNP-binding effects to HSA and HTF by spectroscopic and molecular modeling techniques, J. Biomol. Struct. Dyn. 32 (12) (2014) 1936–1952.
[35] M.M. Alanazi, A.A. Almehizia, A.H. Bakheit, N.A. Alsaif, H.M. Alkahtani, T.A. Wani, Mechanistic interaction study of 5, 6-Dichloro-2-[2-(pyridin-2-yl) ethyl] isoindoline-1, 3-dione with bovine serum albumin by spectroscopic and molecular docking approaches, Saudi Pharm. J. 27 (3) (2019) 341–347.
[36] T.A. Wani, A.H. Bakheit, M.A. Abounassif, S. Zargar, Study of interactions of an anticancer drug neratinib with bovine serum albumin: spectroscopic and molecular docking approach, Front. Chem. 6 (2018) 47.
[37] P. Kandagal, S. Ashoka, J. Seetharamappa, S. Shaikh, Y. Jadegoud, O. Ijare, Study of the interaction of an anticancer drug with human and bovine serum albumin: spectroscopic approach, J. Pharm. Biomed. Anal. 41 (2) (2006) 393–399.